NANO LETTERS

2008
Vol. 8, No. 5
1281-1285

Screening-Limited Response of NanoBiosensors

Pradeep R. Nair* and Muhammad A. Alam*

School of Electrical and Computer Engineering, Purdue University, West Lafayette, Indiana 47907

Received October 8, 2007; Revised Manuscript Received January 28, 2008

ABSTRACT

Despite tremendous potential of highly sensitive electronic detection of biomolecules by nanoscale biosensors for genomics and proteomic applications, many aspects of experimentally observed sensor response (S) are difficult to understand within isolated theoretical frameworks of kinetic response or electrolyte screening. In this paper, we combine analytic solutions of Poisson–Boltzmann and diffusion-capture equations to show that the electrostatic screening within an ionic environment limits the response of nanobiosensor such that $S(t) \sim c_1(\ln(\rho_0) - \ln(l_0)/2 + \ln(t)/D_F + c_2[\mathrm{pH}]) + c_3$ where c_i are geometry-dependent constants, ρ_0 is the concentration of target molecules, l_0 the salt concentration, and D_F the fractal dimension of sensor surface. Our analysis provides a coherent theoretical interpretation of a wide variety of puzzling experimental data that have so far defied intuitive explanation.

1. Introduction. Nanoscale devices have recently been explored for label-free electrical detection of biomolecules. For example, functionalized silicon nanowire (Si-NW) devices have been used to demonstrate detection of DNA[1–3] and proteins[4,5] at very low concentrations. It is generally believed that with improvement in functionalization schemes and scaling of device dimensions, multiplexed detection of biomolecules at very low concentrations and in rapid flux can be achieved. Although tremendous improvements in sensitivity have been reported in electrical detection of biomolecules over the last 5–10 years, many aspects of experimental results are still not well explained within consistent theoretical framework.

The gap between existing theoretical understanding and the reported experiments is particularly evident from the following unexplained observations: (i) Anomalous logarithmic dependence of sensor response on target biomolecule concentration (Figure 2a[1–5]), (ii) linear dependence of sensitivity on pH, which is crucial for protein detection (Figure 2b[5,6]), (iii) nonlinear dependence of sensitivity on electrolyte concentration (Figure 2c[7]), and (iv) logarithmic time-dependence of sensor response instead of the classical Langmuir-type response (Figure 2d[1,2]).

In this paper, we provide a comprehensive theory that interprets the four above-mentioned observations quantitatively and systematically. The theory is based on self-consistent solution of the diffusion-capture model and Poisson–Boltzmann equation, illustrating the importance of screening-limited kinetic response of nanobiosensors. We describe the model equations in Section 2, which are then used to study the screening-limited response of nanobiosensors in Section 3. We conclude in Section 4.

2. Model Equations. A. Kinetics of Biomolecule Adsorbtion. The diffusion-capture model describing the kinetics of biomolecule adsorption on nanosensors (Figure 1a) is given by

$$\frac{\mathrm{d}\rho}{\mathrm{d}t} = D\nabla^2\rho \tag{1a}$$

$$\frac{\mathrm{d}N}{\mathrm{d}t} = k_F(N_0 - N)\rho_S - k_R N \tag{1b}$$

Equation 1a represents the diffusion of target molecules to the sensor surface where ρ is the concentration and D is the diffusion coefficient of target biomolecules (analyte) in solution, respectively. Equation 1b represents the capture of biomolecules by the receptors functionalized on the sensor surface, where N is the density of conjugated receptors, N_0 is the density of receptors on the sensor surface, k_F and k_R are the capture and dissociation constants, and ρ_S is the concentration of analyte particles at the sensor surface.

On the basis of the perturbation approach reported in ref 8, transport limited kinetic response of sensors (solution of eq 1) is given by

$$-\frac{k_F N_0 + E - k_F N_{equi}}{k_F\rho_0 + k_R}\log\left(1 - \frac{N}{N_{equi}}\right) + \frac{k_F}{k_F\rho_0 + k_R}N = Et \tag{2}$$

Here $E = (N_{avo}C_D(t))/A_D$, where N_{avo} is the Avogadro's constant, $C_D(t)$ the time-dependent diffusion equivalent capacitance,[8] A_D the area of sensor surface, and

* Corresponding authors. E-mail: pnair@purdue.edu (P.R.N.); alam@purdue.edu (M.A.A.).

10.1021/nl072593i CCC: $40.75 © 2008 American Chemical Society
Published on Web 04/03/2008

$$N_{\text{equi}} = \frac{k_F N_0 \rho_0}{k_F \rho_0 + k_R} \tag{3a}$$

which is the equilibrium concentration of conjugated molecules. It should be noted that similar solutions are also reported in ref 9, except that ref 9 considers only *steady-state flux to the adsorber*, while here we focus on time dynamics of molecule capture. The solution given by eq 2 is quite general and accurately predicts the diffusion slow down in different types of sensors.

The two limits for N relevant for analysis in Section 3 are: (i) steady-state phase (i.e., $t \rightarrow \infty$), where eq 2 reduces to $N \rightarrow N_{\text{equi}}$ as the *log*-term in eq 2 approaches infinity, and (ii) transient phase (i.e., $t < T_{\text{sat}}$, where T_{sat} is time taken to reach steady state), where eq 2 reduces to the recently reported scaling law for nanoscale sensors[10]

$$N(t) \sim k\rho_0 t^{(1/D_F)} \tag{3b}$$

where k is a geometry dependent constant and D_F is the fractal dimension of the sensor surface.

B. Electrical Response of Biosensor. The conductance modulation of a NW sensor can be derived from a simple capacitor model (see Figure 1c). Charge conservation of the system indicates that

$$\sigma_T = -(\sigma_{DL} + \sigma_{NW}) \tag{4a}$$

where σ_T is the charge density due to analyte molecules on the sensor surface, σ_{DL} is the net charge in the electrical double layer formed at the sensor surface (which represents the screening due to the ions in the electrolyte), and σ_{NW} is the charge induced in the sensor. The charge density due to analyte biomolecules is given by

$$\sigma_T \cong \sigma_S N(t) \tag{4b}$$

where σ_S is the charge of a biomolecule. Note that we have approximated σ_T by the charge due to captured biomolecules only. This approximation applies to high-sensitivity, low-analyte density sensors relevant for modern biosensing applications, where the average analyte molecule spacing is much larger than the Debye-screening length of an electrolyte (discussed below).

The full charge of the captured biomolecules is not effective in modulating the conductance of sensors due to the electrostatic screening of ions present in the electrolyte. To account for screening, one must solve the nonlinear Poisson–Boltzmann equation[11]

$$-\nabla^2\Psi(r) + \frac{\kappa^2}{\beta}\sinh(\beta\Psi) = \frac{q}{\epsilon_W}\sum_i z_i\,\delta(r - r_i) \tag{5}$$

where Ψ is the electrostatic potential, κ^{-1} is the Debye–Huckel screening length and r is the spatial coordinate. $\kappa^2 = 2q^2 I_0 N_{avo}(\epsilon_W k_B T)^{-1}$, where I_0 is the ion concentration in molar units and ϵ_W is the dielectric constant of electrolyte. The sinh term denotes the contribution due to a 1–1 electrolyte (e.g., $Na^+ - Cl^-$), whose ions are assumed to follow Boltzmann distribution ($\beta = q/k_B T$, where q is the electronic charge, k_B is the Boltzmann constant and T is the temperature). The right-hand side denotes the fixed charge due to the biomolecule, z_i and r_i denoting the partial charge and location of the atoms within the biomolecule, respectively (e.g., the phosphate ions in the backbone of a DNA strand).

The double layer charge density σ_{DL}, in terms of the potential at the sensor surface Ψ_0, is given by (analytical solution of eq 5 in cylindrical coordinates in an infinite media, without a sensor nearby[12])

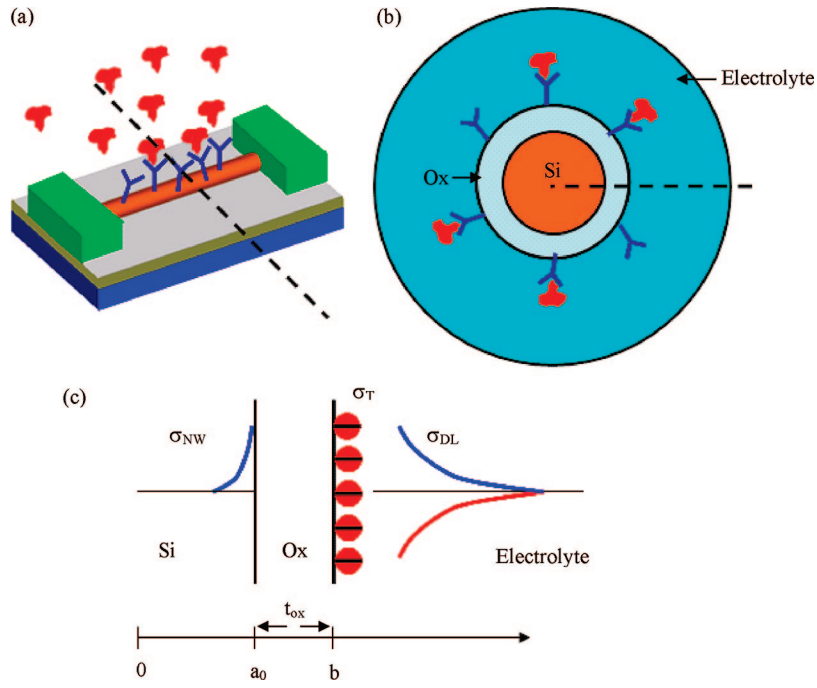

Figure 1. Schematic of nanoscale biosensor. (a) NW surface is functionalized with receptors for target biomolecules. (b) Cross-section of the sensor along the dotted line shown in (a). (c) Charge distribution in the sensor system along the dotted line shown in (b). Device parameters are also indicated.

$$\sigma_{DL} = -\frac{2\epsilon_W \kappa}{\beta} \sinh(\beta\Psi_0/2)\left(1 + \frac{\gamma^{-2} - 1}{\cosh^2(\beta\Psi_0/2)}\right)^{1/2} \quad (6a)$$

where $\gamma = (K_0(\kappa b))/(K_1(\kappa b))$, K_n is the modified Bessel function of the second kind of order n, and $b = a + t_{ox}$, a the radius of NW, and t_{ox} the oxide thickness (see Figure 1b,c). Equation 6a shows that the amount of charge shared by the electrolyte increases exponentially with the surface potential and this electrolyte screening reduces the electrical response of nanobiosensors. Analytic solutions of eq 5 are also available for other systems,[13,14] and the methodology of this section can easily be extended to them as well.

The induced charge density of a heavily doped cylindrical NW can be calculated (see Figure 1b,c) by using the formula for capacitance of oxide dielectric on cylindrical NW, i.e.,

$$\sigma_{NW} = -\frac{\epsilon_{ox}}{b \log\left(1 + \frac{t_{ox}}{a}\right)}\Psi_0 \quad (6b)$$

By combining eqs 4 and 6, we have

$$\frac{\epsilon_{ox}}{b \log(1 + t_{ox}/a)}\Psi_0 + \frac{2\epsilon_W \kappa}{\beta} \sinh(\beta\Psi_0/2)\left(1 + \frac{\gamma^{-2} - 1}{\cosh^2(\beta\Psi_0/2)}\right)^{1/2} = \sigma_S N(t) \quad (7)$$

Equation 7 represents the charge conservation of the system.

The electrical response is proportional to σ_{NW} and hence also to Ψ_0 (solution of eq 7). On the basis of ref 15, the sensor response (relative change in conductance) is given by $S = \Delta G/G_0 = 2\sigma_{NW}/qN_D a$, where G is the conductance and N_D is the doping density. The sensitivity S, in terms of Ψ_0 and other device parameters, is given as

$$S = \frac{2\epsilon_{ox}\Psi_0(N(t))}{qa^2 N_D \log\left(1 + \frac{t_{ox}}{a}\right)} \quad (8)$$

Equations 2, 7, and 8 allow us to compute $S(t)$ self-consistently. Note that the ultimate, ideal performance limit of sensor response, as discussed in refs 8, 10 is obtained if screening of the target molecule approaches zero ($I_0 \rightarrow 0$ or equivalently $\kappa \rightarrow 0$). In this limit, eq 7 indicates that $\Psi_0 = \sigma_S N(t)\ b\log(1 + t_{ox}/a)/\epsilon_{ox}$. By substituting Ψ_0 in eq 8, we find that the ideal performance limit of sensor response is given by $S = ((2\pi b)(\sigma_s N))/((\pi a^2)(qN_D))$, which involves the ratio of adsorbed charge to the total doping of the NW, an intuitive result.

3. Application of Model. The self-consistent screening-limited kinetic response of nanobiosensors may be obtained by solving eqs 2, 7, and 8 numerically. In this section, we decompose the problem into steady-state and transient solutions and then provide approximate analytic solutions that can provide considerable insight into the details of nanoscale biosensor response. All approximate analytical solutions are checked against exact numerical solutions for accuracy (using eqs 2, 7, and 8).

A. Steady-State Response due to Target Molecule. The steady-state response can be obtained by replacing $N(t)$ in the right-hand side of eq 7 with N_{equi}. At low analyte concentrations (i.e., if $k_F\rho_0 \ll k_R$), N_{equi} can be approximated as $N_{equi} = (k_F/k_R)N_0\rho_0$ (see eq 3a). At low electrolyte concentrations (to maximize sensitivity), Ψ_0 due to highly charged biomolecules like DNA satisfy the relation $\Psi_0 > 1/\beta$ even up to multiple mM concentrations (from numerical solution of eq 5[15]). Under these conditions, an approximate solution of Ψ_0 can be obtained from eq 7. Neglecting the first term of eq 7 and using the limits $Lt_{x\rightarrow\infty} \sinh(x) = e^x/2 = Lt_{x\rightarrow\infty} \cosh(x)$, we find $2\epsilon_W\kappa/\beta \sinh(\beta\Psi_0/2) \approx \sigma_S N_{equi} = \sigma_S k_F/k_R N_0\rho_0$, or equivalently

$$\Psi_0 = \frac{2}{\beta}\left[\ln(\rho_0) - \frac{\ln(I_0)}{2} + c_2\right] \quad (9)$$

where $c_2 = \ln((\sigma_S k_F N_0/k_R)(\beta/q^3\epsilon_w N_{avo})^{1/2})$. Inserting Ψ_0 in eq 8 gives the sensor response

$$S(t) = c_1\left[\ln(\rho_0) - \frac{\ln(I_0)}{2} + c_2\right] \quad (10)$$

where $c_1 = 4\epsilon_{ox}/\beta q a^2 N_D \log(1 + t_{ox}/a)$.

Equation 10 shows that nanoscale sensors show logarithmic dependencies on the target molecule concentration ρ_0 and the electrolyte concentration I_0 due to the inherent nonlinear screening by the electrolyte of the system. *This theoretical explanation resolves the puzzle of log dependence of electrical response on target biomolecule concentration (see the list of four puzzles in Section 1).*[16] This is in contrast with classical theory (eq 2) and fluorescence measurements,[10] which indicate linear dependence on analyte concentration. Numerical solution of eqs 7 and 8 using N_{equi} for the equilibrium concentration of captured molecules also shows the same trend (see Figure 2a), validating our analytical approach.

There are several noteworthy features in eq 10 and Figure 2a: First, the slope of $S(t)$ vs $\log(\rho_0)$ depends on the device parameters (c_1 in eq 10) and parasitic contact resistances. Inset of Figure 2a (simulations) shows a comparison of the theoretical and experimental slopes of $S(t)$ vs $\log(\rho_0)$. The predictions from the analytic model compares well with the experimental results, given the uncertainties in the doping density of NW devices and the effect of parasitic contact resistances (neglected in analytical model). Second, the range of analyte concentration over which the log dependence is observed can be obtained in simple terms: For $k_F\rho_0 \gg k_R$, N_{equi} is independent of ρ_0. This provides an upper bound of ρ_0 for linear−log dependence of sensor response, i.e., $\rho_{0,max} = k_R/k_F$. Sensor response will vary logarithmically with ρ_0 until $\Psi_0 > 1/\beta$, leading to the lower bound of ρ_0, i.e., $\rho_{0,min} = (2\epsilon_W\kappa k_R e^2)/(10\beta\sigma_S k_F N_0)$. It is interesting to note that while $\rho_{0,max}$ is entirely determined by the reaction coefficient, $\rho_{0,min}$ is also influenced by the system parameters. For typical parameters, the ratio $\rho_{0,max}/\rho_{0,min}$ predicts a range of 10^2-10^4, which agrees well with the experimental data (see Figure 2a).

B. Steady-State pH Detection. The theoretical framework described in Section 3A can also be used to determine the sensor response to fluctuations in pH of the solution. The net charge density (right-hand side of eq 7) on the NW surface can be obtained based on first-order chemical kinetics of bond dissociation for the particular type of surface functionalization schemes used (−OH, $-NH_2$, etc.[6]). Beyond pK_a (p$K_a = -\log_{10}(K_a)$, K_a the dissociation constant) of the

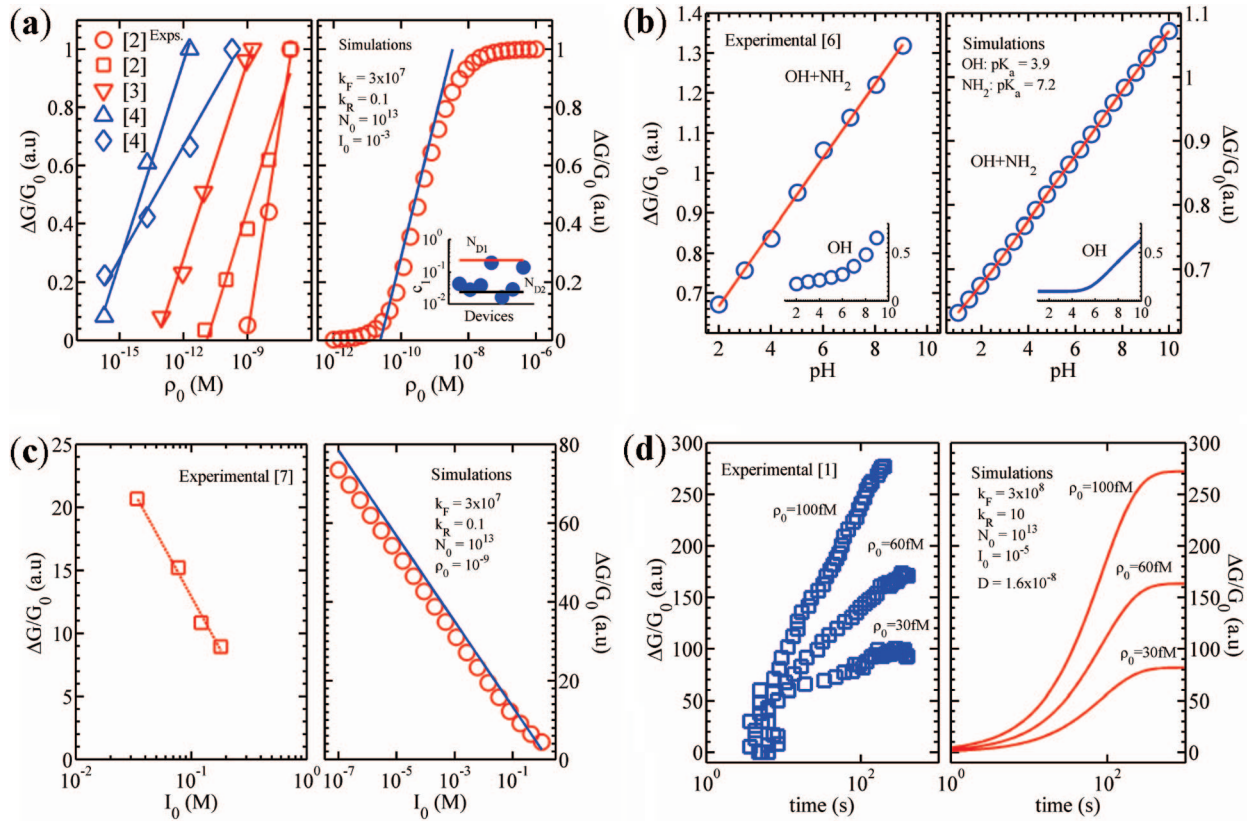

Figure 2. Comparison between experimental (left panel) and simulated response (right panel) of nanobiosensors. (a) Variation with analyte concentration: *logarithmic dependence on* ρ_0. Experimental data has been normalized. The inset in right panel shows the comparison of theoretical slope c_1 with experimental results ($N_{D1} = 10^{19}$ cm^{-3}, $N_{D2} = 10^{20}$ cm^{-3}. Experimental N_D is of the order of 10^{19} cm^{-3}). (b) Variation of sensitivity with pH (surface functionalized with amide and OH groups): *linear dependence on pH*. Inset shows the response with only OH groups. (c) Variation of response with ion concentration of electrolyte:*logarithmic dependence on* I_0. (d) Transient response of nanobiosensors: *logarithmic dependence on time*. The units of various simulation parameters are: k_F (M^{-1} s^{-1}), k_R (s^{-1}), N_0 (cm^{-2}), ρ_0 (M), I_0 (M), and D (cm^2/s). For simulations, the symbols represent numerical results, while the solid lines represent analytical results. Surface potential Ψ_0 varies from 0 to –135 mV in (a), –218 to 222 mV in (b) and −400 to –20 mV in (c) for the parameters used in corresponding simulations.

particular functionalization group, the net charge density on the sensor surface is given as $\sigma_{pH} \approx qN_F\, e^{(\beta\Psi_0 + 2.303(pH - pK_a))}$, where N_F is the density of surface functionalization groups.[18,19] Replacing $\sigma_S N(t)$ (right-hand side of eq 7) by σ_{pH} and then repeating the derivation from Section 3A, we find

$$S(t) = c_1\left[2.303\alpha \times |pH - pK_a| - \frac{\ln(I_0)}{2} + c_3\right] \qquad (11)$$

where α and c_3 are constants such that the response of sensors vary linearly with pH of solution ($0 \le \alpha \le 0.5$). The theoretical limit for the maximum rate of change of surface potential with pH ($(\partial\Psi_0/\partial pH)_{max} = 60$ mV/pH) predicted by the model agrees well with the results in literature.[18] Numerical solution of eqs 7 and 8 in the presence of different surface functionalization groups (−OH and −NH$_2$) shows that linear response can be obtained over a wide range of pH (Figure 2b, inset indicates the response in the presence of −OH groups only), in general agreement with the reported experimental results.

C. Steady-State Response with Various Electrolyte Concentration. Dependence of sensor response to variations in salt concentration of the electrolyte is of paramount interest in deciding the surface functionalization schemes.[16] Equation 10 indicates that, for a given analyte density, ρ_0, the sensitivity reduces logarithmically with the ion concentration, I_0, also observed experimentally (see Figure 2c). This is intuitively obvious because screening by the ions suppresses the overall charge effective in modulating the sensor response. Numerical solution of eqs 7 and 8, for different I_0, shown in Figure 2c, support the experimental results very well. Finally, our results indicate the critical importance of optimizing the electrolyte concentration in experiments involving biosensors because the same target molecules may result in different sensitivity depending on the ion concentration.

D. Screening-Limited Transient Response of Biosensors. The transient response can be obtained by replacing $N(t)$ in the right-hand side of eq 7 with eq 3b. Following the same derivation methodology as in Section 3A, we get

$$S(t) = c_1\left[\ln(\rho_0) + \frac{\ln(t)}{D_F} - \frac{\ln(I_0)}{2} + c_4\right] \qquad (12)$$

Equation 12 indicates that electrostatic screening converts the pure power-law kinetic response of biosensors (4b) to a logarithmic dependence in time, scaled by sensor-specific fractal dimension. This is intuitively reasonable because one can view the time-dependence of molecule arrival equivalently as a series of steady-state responses of a sensor with

increasing analyte concentration. Because steady-state response is logarithmic, so is the time-dependence. The predicted trends have also been observed experimentally (Figure 2d).

4. Discussions A. Performance Limits of Sensors. The detection limits of nanoscale sensors in a diffusion limited regime are predicted by eq 12. However, screening due to the ions can significantly increase the average incubation times for achieving the same sensor response. This is evident from eq 12. An increase in 2 orders of magnitude of ion concentration (e.g., from 1 mM to 0.1M) increases the average *electrical* settling time for cylindrical NW sensors ($D_F = 1$) by 1 order of magnitude, while that of planar sensors ($D_F = 2$) increases by 2 orders of magnitude. Hence it is important to develop functionalization schemes at low ion concentrations not only due to the electrostatic screening of ions (magnitude of sensor response) but also to reduce the time taken for obtaining a detectable signal change. Equation 12 also implies that, due to electrostatic screening, the settling times scale exponentially with device parameters.

B. Extraction of Reaction Coefficients. Response of nanoscale sensors has often been used to extract the reaction coefficients k_F and k_R by fitting the observed experimental response with the solution of eq 1b without accounting for the diffusion induced delay[2] or the nonlinear transformation between the density of captured molecules and the measured signal. Our theory, for the first time, provides a self-consistent method of characterizing the surface reaction coefficients from the electrical response of a sensor in a diffusion limited regime (using eqs 2, 7, and 8).

C. Surface Potential and Induced Charge. It should be noted that the origin of logarithmic dependencies of sensor response on various parameters like ρ_0, I_0, and t are due to the fact that the surface potential Ψ_0 is such that $\Psi_0 > 1/\beta$. If the number or the net charge of biomolecules captured on the sensor surface is very small (which makes Ψ_0 comparable to $1/\beta$), as per eqs 2, 7, and 8, the sensor response is expected to vary linearly with each of these parameters. However, the condition $\Psi_0 > 1/\beta$ is satisfied by highly charged biomolecules like DNA, even up to multiple mM electrolyte concentrations.[15] Also, in this paper, we discussed the response of nanoscale biosensors in the linear transport regime (eq 8), where the response varies linearly with the surface potential Ψ_0. If the device is operated in nonlinear regime (e.g., subthreshold of FETs, where the conduction varies exponentially with Ψ_0), eq 8 would have to be modified as $S \propto e^{\beta\Psi_0}$. In such a regime, the sensor response could vary linearly with parameters like ρ_0, I_0, and time. Moreover, in the subthreshold regime, response could vary exponentially with pH.[20] Other parameters and issues relevant for sensor design are discussed in ref 15.

To summarize, the theory of nanoscale biosensor response, based on analytic solutions of Poisson–Boltzmann and reaction-diffusion equations, is discussed. Specifically, our model predicts that the sensor response varies (a) logarithmically with target biomolecule concentration, (b) linearly with pH, (c) logarithmically with the electrolyte concentration, and (d) the transient response varies logarithmically with time. The theoretical predictions agree well with experimental results and have important implications for the design and optimization of nanoscale biosensors.

Note Added after ASAP Publication: This paper was published ASAP on April 3, 2008. An in-line equation in Section 3B was updated. The revised paper was reposted on April 15, 2008.

References

(1) Hahm, J.; Leiber, C. M. *Nano. Lett.* **2004**, *4*, 51–55.
(2) Bunimovich, Y. L.; Shin, Y. S.; Yeo, W.; Amori, M.; Kwong, G.; Heath, J. R. *J. Am. Chem. Soc.* **2006**, *128*, 16323–16331.
(3) Cheng, M. M.; Cuda, G.; Bunimovich, Y. L.; Gaspari, M.; Heath, J. R.; Hill, H. D.; Mirkin, C. A.; Nijdam, A. J.; Terraciano, R.; Thundat, T.; Ferrari, M *Curr. Opin. Chem. Biol.* **2006**, *10*, 11–19.
(4) Zheng, G.; Patlowsky, F.; Cui, Y.; Wang, W. U.; Lieber, C. M. *Nat. Biotechnol.* **2005**, *23*, 1294–1301.
(5) Stern, E.; Klemic, J. F.; Routenberg, D. A.; Wyrembak, P. N.; Turner-Evans, D. B.; Hamilton, A. D.; LaVan, D. A.; Fahmy, T. M.; Reed, M. A. *Nature* **2007**, *445*, 519–523.
(6) Cui, Y.; Wei, Q.; Park, H.; Lieber, C. M. *Science* **2001**, *293*, 1289–1292.
(7) Lud, S. Q.; Nikolaides, M. G.; Haase, I.; Fisher, M.; Baush, A. R. *ChemPhysChem* **2006**, *7*, 379–384.
(8) Nair, P. R.; Alam, M. A. *Appl. Phys. Lett.* **2006**, *88*, 233021–233023.
(9) Kusnezow, W.; Syagailo, Y.; Rüffer, S.; Klenin, K.; Sebald, W.; Hoheisel, J. D.; Gauer, C.; Goychuk, I. *Proteomics* **2006**, *6*, 794–803.
(10) Nair, P. R.; Alam, M. A. *Phys. Rev. Lett.* **2007**, *99*, 256101.
(11) McQuarrie, D. *Statistical Mechanics*; New York: Harper & Row, 1976.
(12) Ohshima, H. *J. Colloid Interface Sci.* **1998**, *200*, 291–298.
(13) Grahame, D. C. *Chem. Rev.* **1947**, *41*, 441–501.
(14) White, L. R. *J. Chem. Soc., Faraday Trans. 2* **1977**, *73*, 577–596.
(15) Nair, P. R.; Alam, M. A. *IEEE Trans. Electron Devices* **2007**, *54*, 3400–3408.
(16) Steady-state response of planar systems is previously discussed in ref 17 (protein detection) and refs 18, 19 (pH sensors).
(17) Bergveld, P. *Biosens. Bioelectron.* **1991**, *6*, 55–72.
(18) Bergveld, P.; van Hal, R. E. G; Eijkel, J. C. T. *Biosens. Bioelectron.* **1995**, *10*, 405–414.
(19) Fung, C. D.; Cheung, P. W; Ko, W. H. *IEEE Trans. Electron Devices* **1986**, *33*, 8–18.
(20) Elibol, O. H.; Reddy, J.; Bashir, R. *Nano Lett.*, under review.

NL072593I